Synthesis and Reactions of Heterodinuclear Organoplatinum Complexes Having an Unsymmetrical PN Ligand

Susumu Tsutsuminai, Nobuyuki Komine, Masafumi Hirano, and Sanshiro Komiya*

Department of Applied Chemistry, Faculty of Technology, Tokyo University of Agriculture and Technology, 2-24-16 Nakacho, Koganei, Tokyo 184-8588, Japan

Received June 20, 2003

A series of heterodinuclear organoplatinum complexes having an unsymmetrical PN ligand ($Et_2NC_2H_4PPh_2$-κ^2N,P)RPt−ML_n [ML_n = $MoCp(CO)_3$, R = Me (**1**), R = Ph (**2**); ML_n = $WCp(CO)_3$, R = Me (**3**), R = Ph (**4**); ML_n = $Co(CO)_4$, R = Me (**5**), R = Ph (**6**)] have been synthesized by metathetical reactions of $PtR(NO_3)(Et_2NC_2H_4PPh_2$-$\kappa^2N,P)$, which is prepared in situ from $PtRCl(Et_2NC_2H_4PPh_2$-$\kappa^2N,P)$ (R = Me, Ph) and $AgNO_3$, with Na[ML_n]. Analogous complexes with a bidentate nitrogen ligand (tmeda-κ^2N,N')RPt−$MoCp(CO)_3$ [R = Me (**7**), Ph (**8**)] are also prepared by ligand exchange reaction of (cod)RPt−$MoCp(CO)_3$ with TMEDA (*N*,*N*,*N*′,*N*′-tetramethylethylenediamine). These complexes are characterized by NMR and IR spectroscopies and elemental analyses, and the molecular structure of **2** is determined by X-ray structure analysis. Variable-temperature NMR study reveals the reversible partial dissociation of the Pt−N bond in **2** and **4**, where the kinetic parameters are estimated by line shape analysis of **2**: $\Delta G_{273}^{\ddagger}$ = 57.9 kJ mol^{-1}, $\Delta H^{\ddagger}$= 49.8 kJ mol^{-1}, $\Delta S^{\ddagger}$ = −29.7 J mol^{-1} K^{-1}. Treatment of **1**−**4** with CO causes partial dissociation of the amino ligand moiety in the PN ligand from the Pt center to form ($Et_2NC_2H_4PPh_2$-κ^1P)(CO)RPt−$MCp(CO)_3$ [M = Mo, R = Me (**9**), Ph (**10**); M = W, R = Me (**11**), Ph (**12**)]. Heating of **9** at 70 °C induces CO insertion to give an equilibrium mixture of ($Et_2NC_2H_4PPh_2$-κ^2N,P)(MeCO)Pt−$MoCp(CO)_3$ (**14**) with **9** in 3:2 ratio. In contrast, the Pt−Co complex **5** with a PN ligand smoothly yields the acetyl complex ($Et_2NC_2H_4PPh_2$-κ^2N,P)(MeCO)Pt−$Co(CO)_4$ (**15**) on interaction with CO at room temperature. On the other hand, in the reactions of **1** with $Et_2NC_2H_4PPh_2$ or phosphorus ligand such as PMe_3, PEt_3, PPh_3, and $P(OMe)_3$, heterolytic cleavage of the Pt−Mo bond takes place to give ionic complexes [$PtMe(PR_3)(Et_2NC_2H_4PPh_2$-$\kappa^2N,P)]^+[MoCp(CO)_3]^-$ [PR_3 = $Et_2NC_2H_4PPh_2$ (**17**), PMe_3 (**18**), PEt_3 (**19**), PPh_3 (**20**), $P(OMe)_3$ (**21**)].

Introduction

Heterodinuclear complexes attract intrinsic interest due to their possible cooperative effect of two different metal centers in catalytic and stoichiometric chemical reactions.[1,2] We previously reported the synthesis of heterodinuclear organoplatinum or -palladium complexes containing a symmetrical bidentate ligand L_2-RM−M′L_n (L_2 = cod, dppe, tmeda, bpy, phen; R = alkyl, aryl; M = Pt, Pd; M′L_n = $MoCp(CO)_3$, $WCp(CO)_3$, $Mn(CO)_5$, $Re(CO)_5$, $FeCp(CO)_2$, $Co(CO)_4$).[3,4] They show unique reactions such as specific organic group transfer between different metal centers,[4a−c,f,h] significant acceleration of β-H elimination,[4d] accelerated CO insertion reactions,[4e,i] and regio- and stereoselective insertion reactions of thiiranes into Pt−Mn (or −Re) bonds controlled by an ancillary alkyl ligand.[4g] Introduction of an unsymmetrical PN chelating ligand into such dinuclear complexes is expected to provide a highly selective reaction environment, because preferential dissociation of the PN chelating ligand gives a specific vacant coordination site on a metal center due to facile dissociation of the nitrogen atom.[5] In this paper, we wish to report the synthesis of novel heterodinuclear organoplatinum complexes having an unsymmetrical PN ligand [2-(diphenylphosphino)triethylamine], where

* Corresponding author.

(1) (a) Braunstein, P., Oro, L. A., Raithby P. R., Eds. *Metal Clusters in Chemistry*; Wiley-VCH: Weinheim, Germany, 1999. (b) Adams, R. D., Cotton, F. A., Eds; *Catalysis by Di- and Polynuclear Metal Cluster Complexes*; Wiley-VCH: New York, 1998. (c) Chetcuti, M. J. In *Comprehensive Organometallic Chemistry II*; Adams, R. D., Ed.; Pergamon Press: Oxford, U.K., 1995; Vol. 10. (d) Shriver, D. F., Kaesz, H., Adams, R. D., Eds. *The Chemistry of Metal Cluster Complexes*; VCH: New York, 1990.

(2) (a) Braunstein, P.; Morise, X. *Organometallics* **1998**, *17*, 540. (b) Adams, R. D.; Barnard, T. S.; Wu, Z. Li. W.; Yamamoto, J. H. *J. Am. Chem. Soc.* **1994**, *116*, 9103. (c) Braunstein, P.; Knorr, M.; Stähreldt, J. *J. Chem. Soc., Chem. Commun.* **1994**, 1913.

(3) Abbreviations used in this article: cod = 1,5-cyclooctadiene (C_8H_{12}), dppe = 1,2-bis(diphenylphosphino)ethane ($Ph_2PC_2H_4PPh_2$), tmeda = *N*,*N*,*N*′,*N*′-tetramethylethylenediamine ($Me_2NC_2H_4NMe_2$). Free ligands are expressed by capital letters.

(4) (a) Komiya, S.; Endo, I. *Chem. Lett.* **1988**, 1709. (b) Fukuoka, A.; Sadashima, T.; Endo, I.; Ohashi, N.; Kambara, Y.; Sugiura, T.; Komiya, S. *Organometallics* **1994**, *13*, 4033. (c) Fukuoka, A.; Sadashima, T.; Sugiura, T.; Wu, X.; Mizuho, Y.; Komiya, S. *J. Organomet. Chem.* **1994**, *473*, 139. (d) Fukuoka, A.; Sugiura, T.; Yasuda, T.; Taguchi, T.; Hirano, M.; Komiya, S. *Chem. Lett.* **1997**, 329. (e) Fukuoka, A.; Fukagawa, S.; Hirano, M.; Komiya, S. *Chem. Lett.* **1997**, 377. (f) Yasuda, T.; Fukuoka, A.; Hirano, M.; Komiya, S. *Chem. Lett.* **1998**, 29. (g) Komiya, S.; Muroi, S.; Furuya, M.; Hirano, M. *J. Am. Chem. Soc.* **2000**, *122*, 170. (h) Komine, N.; Hoh, H.; Hirano, M.; Komiya, S. *Organometallics* **2000**, *19*, 5251. (i) Fukuoka, A.; Fukagawa, S.; Hirano, M.; Koga, N.; Komiya, S. *Organometallics* **2001**, *20*, 2065.

10.1021/om030477u CCC: $25.00
Publication on Web 09/16/2003

Scheme 1

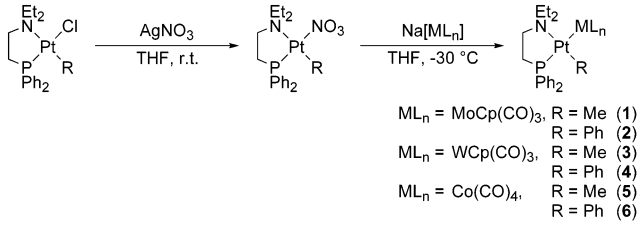

reversible dissociation of the nitrogen atom is observed by VT NMR. Facile insertion of carbon monoxide into the Pt−C bond is demonstrated for these heterodinuclear complexes with a hemilabile PN ligand.

Results and Discussion

Synthesis and Characterization of Heterodinuclear Organoplatinum Complexes Having an Unsymmetrical PN Ligand. Heterodinuclear organoplatinum complexes having an unsymmetrical PN ligand were prepared by the metathetical reaction of $PtRCl(Et_2NC_2H_4PPh_2$-$\kappa^2N,P)$ (R = Me, Ph) with various carbonylmetallates. Starting complexes $PtRCl(Et_2NC_2H_4PPh_2$-$\kappa^2N,P)$ were prepared by the ligand exchange reaction of PtRCl(cod) with 2-(diphenylphosphino)triethylamine. The $^{31}P\{^1H\}$ NMR spectrum of $PtMeCl(Et_2NC_2H_4PPh_2$-$\kappa^2N,P)$ shows a singlet at δ 27.4 with a large $^1J_{Pt-P}$ value of 4862 Hz, suggesting that the phosphorus atom is located in a position trans to the Cl ligand, which has a smaller trans influence than the Me ligand. In the ^1H NMR of $PtMeCl(Et_2NC_2H_4PPh_2$-$\kappa^2N,P)$, the methylene protons of the NCH_2CH_3 moiety appear as two doublets of quartets at δ 3.14 and 3.40, indicating that these methylene protons are diastereotopic. The fact is an indication of rigid coordination of both nitrogen and phosphorus atoms to the Pt center. The Pt-Me resonance is observed at δ 0.58 as a doublet with a ^{195}Pt satellite ($^3J_{P-H}$ = 4.2 Hz, $^2J_{Pt-H}$ = 76.0 Hz). These spectroscopic data are comparable to that of a similar complex, $PtMeI(Me_2NC_2H_4PPh_2$-$\kappa^2N,P)$, reported by Schubert et al.[5g] Thus the starting complex $PtMeCl(Et_2NC_2H_4PPh_2$-$\kappa^2N,P)$ has a square-planar geometry, as depicted in eq 1. Analogous spectroscopic data are also obtained for $PtPhCl(Et_2NC_2H_4PPh_2$-$\kappa^2N,P)$. Metathetical reactions of $PtR(NO_3)(Et_2NC_2H_4$-

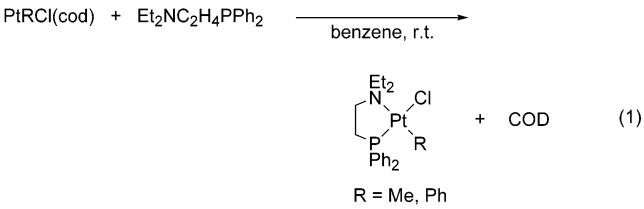

PPh_2-$\kappa^2N,P)$, prepared in situ from $PtRCl(Et_2NC_2H_4$-PPh_2-$\kappa^2N,P)$ and $AgNO_3$, with excess amounts of $Na[ML_n]$ in THF at −30 °C gave novel heterodinuclear organoplatinum complexes having an unsymmetrical PN ligand, $(Et_2NC_2H_4PPh_2$-$\kappa^2N,P)RPt-ML_n$ [ML_n = $MoCp(CO)_3$, R = Me (**1**), R = Ph (**2**); ML_n = $WCp(CO)_3$, R = Me (**3**), R = Ph (**4**); ML_n = $Co(CO)_4$, R = Me (**5**), R = Ph (**6**)] (Scheme 1).

Single crystals of complex **2** suitable for X-ray structure analysis were obtained by recrystallization from toluene/hexane. The crystallographic data and selected bond distances and angles are summarized in Tables 1 and 2, respectively, and an ORTEP drawing is depicted in Figure 1.

The geometry around Pt in **2** is square planar, and the Mo has a three-leg piano-stool type structure. These structural features around both metals are consistent with the electronic configurations of d^8 Pt(II) and d^6 Mo(0), since d^8 complexes normally take a square-planer geometry, and it is known that Mo(0) anionic complex $[MoCp(CO)_3]^-$ has a three-leg piano-stool type structure, but Mo(II) complexes[6] such as $MoCl(CO)_2(Ph_2PN(Me)$-$CH(Me)(Ph))$[6b] and $MoClCp(CO)_3$[6c] usually have a four-leg piano-stool type structure. The IR data also support this electronic configurations (vide infra). The Pt−Mo bond distance is 2.8989(9) Å, which is in a typical range of Pt−Mo single bonds reported for dinuclear and cluster complexes such as $(cod)PhPt-MoCp(CO)_3$ [2.8320(12) Å],[4b] $Cp_2Mo_2Pt(\mu$-$PPh_2)(CO)_5$ [2.860(2), 2.872(2) Å],[7] and $[CpMo(CO)_2(\mu$-dppm$)Pt($dppm$)]^+$ [2.912(4) Å].[8]

Among three carbonyl ligands of Mo, two of them (C(25)−O(1) and C(26)−O(2)) coordinate to the Pt center from both above and below the Pt coordination plane. The Mo(1)−C(25)−O(1) [162.6(9)°] and Mo(1)−C(26)−O(2) [167.1(7)°] linkages are slightly bent, and Pt(1), C(25), Mo(1), and C(26) are located in the same plane. These facts imply that these two CO ligands have weak interactions with Pt. This semibridging carbonyl group[9] was also observed in some heterodinuclear complexes such as $(tmeda)Cu-MoCp(CO)_3$[9b] and $(Ph_3P)_2Rh-MoCp(CO)_3$.[9c]

IR spectra of Pt−Mo or Pt−W complexes (**1**−**4**) show strong ν(CO) bands at ca. 1750−1900 cm^{-1}, which are similar to those for the known M(0) complexes $[MoCp(CO)_3]^-$ and $[WCp(CO)_3]^-$ rather than M(II) complexes $MoMeCp(CO)_3$ and $WMeCp(CO)_3$.[4b,10a,b] Complexes **5** and **6** also show similar ν(CO) bands (1867−2026 cm^{-1}) for the Co(−I) complex $[Co(CO)_4]^-$.[4c,i,10b] These data also suggest that the oxidation states of the platinum and connecting metals in **1**−**6** are likely to be Pt(II) and M(0) (M = Mo, W) or Co(−I), although the formal oxidation states are Pt(I) and M(I) (M = Mo, W) or Pt(I) and Co(0).

The $^{31}P\{^1H\}$ NMR spectra of these complexes show a singlet with ^{195}Pt satellites having a large $^1J_{Pt-P}$ value (ca. 4000−4600 Hz), suggesting that the phosphorus atom of the PN ligand is located in a trans position to

(5) (a) Braunstein, P.; Naud, F. *Angew. Chem., Int. Ed.* **2001**, *40*, 680. (b) Anderson, G. K.; Lumetta, G. J. *Organometallics* **1985**, *4*, 1542. (c) Dekker, G. P. C. M.; Buijs, A.; Elsevier, C. J.; Vrieze, K.; Smeets, W. J. J.; Spek, A. L.; Wang, Y. F.; Stam, C. H. *Organometallics* **1992**, *11*, 1937. (d) Mauthner, K.; Slugovc, C.; Mereiter, K.; Schmid, R.; Kirchner, K. *Organometallics* **1997**, *16*, 1956. (e) Hayashi, T.; Kumada, M. *Acc. Chem. Res.* **1982**, *15*, 395. (f) Yoshida, H.; Shirakawa, E.; Kurahashi, T.; Nakao, Y.; Hiyama, T. *Organometallics* **2000**, *19*, 5671. (g) Pfeiffer, J.; Kickelbick, G.; Schubert, U. *Organometallics* **2000**, *19*, 62. (h) Müller, C.; Lachicotte, R. J.; Jones, W. D. *Organometallics* **2002**, *21*, 1975.

(6) (a) Poli, R. *Organometallics* **1990**, *9*, 1892. (b) Rxisner, G. M.; Berkal, I. *J. Chem. Soc., Chem. Commun.* **1978**, 691. (c) Bueno, C.; Churchll, M. R. *Inorg. Chem.* **1981**, *20*, 2197.

(7) Blum, T.; Braunstein, P. *Organometallics* **1989**, *8*, 2504.

(8) Braunstein, P.; Bellefon, C. M.; Lanfranchi, M.; Tiripicchio, A. *Organometallics* **1984**, *3*, 1772.

(9) (a) Crabtree, R. H.; Lavin, M. *Inorg. Chem.* **1986**, *25*, 805. (b) Doyle, G.; Eriksen, A. *Organometallics* **1985**, *4*, 2201. (c) Carlton, L.; Lindsell, W. E.; McCullough, K. J.; Preston, P. N. *J. Chem. Soc., Dalton Trans.* **1984**, 1693. (d) Sargent, A. L.; Hall, M. B. *J. Am. Chem. Soc.* **1989**, *111*, 1563.

Table 1. Crystal Data for 2 and 21

	2·C_7H_8	**21**
empirical formula	$C_{39}H_{42}MoNO_4PPt$	$C_{30}H_{41}MoNO_6P_2Pt$
fw	894.77	864.63
cryst dimens (mm)	0.36 × 0.27 × 0.27	0.60 × 0.56 × 0.28
cryst syst	triclinic	triclinic
lattice params		
a (Å)	12.329(3)	12.895(10)
b (Å)	13.802(2)	12.975(6)
c (Å)	11.781(4)	11.403(4)
α (deg)	97.88(2)	99.80(3)
β (deg)	111.88(2)	95.46(5)
γ (deg)	80.27(2)	115.16(5)
V (Å^3)	1827.4(9)	1671(1)
space group	$P\bar{1}$ (No. 2)	$P\bar{1}$ (No. 2)
Z value	2	2
D_{calc} (g cm^{-3})	1.626	1.718
F_{000}	884.00	852.00
μ(Mo Ka) (cm^{-1})	42.31	46.74
radiation	Mo Ka (λ = 0.71069 Å) graphite monochromated	Mo Ka (λ = 0.71069 Å) graphite monochromated
tempareture (°C)	−33.0	20.0
scan type	ω-2θ	ω-2θ
$2\theta_{max}$ (deg)	55.0	55.0
no. of reflns measd	8712	8007
no. of unique reflns	8364 (R_{int} = 0.022)	7666 (R_{int} = 0.023)
structure solution	direct methods	direct methods
no. of observations ($I > 3.00\sigma(I)$)	6228	6660
no. of variables	334	370
residuals: R^a; $R_w{}^b$	0.048; 0.066	0.029; 0.046
GOF	1.08	1.51

^{a} $R = \sum||F_o| - |F_c||/\sum|F_o|$. ^{b} $R_w = [\sum w(|F_o| - |F_c|)^2/\sum wF_o^2]^{1/2}$.

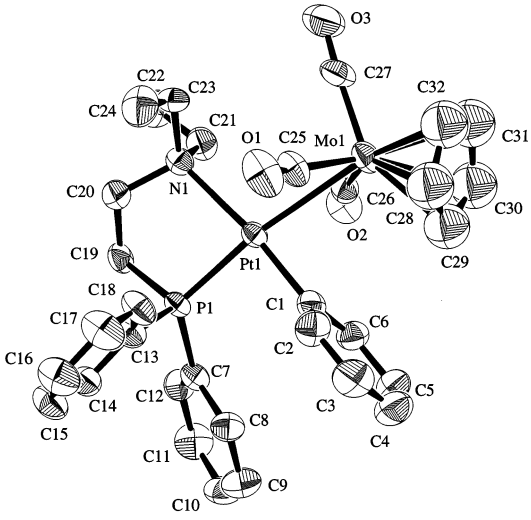

Figure 1. ORTEP drawing of ($Et_2NC_2H_4PPh_2$-κ^2N,P)-PhPt−$MoCp(CO)_3$ (**2**). All hydrogen atoms and solvent are omitted for clarity. Ellipsoids represent 50% probability.

Table 2. Selected Bond Lengths and Angles for 2

Bond Lengths (Å)			
Pt(1)−Mo(1)	2.8989(9)	Pt(1)−C(1)	2.001(9)
Pt(1)−P(1)	2.253(2)	Pt(1)−N(1)	2.330(6)
Mo(1)−C(25)	1.979(8)	Mo(1)−C(26)	1.975(10)
Mo(1)−C(27)	1.92(1)	C(25)−O(1)	1.16(1)
C(26)−O(2)	1.17(1)	C(27)−O(3)	1.18(2)

Bond Angles (deg)			
Mo(1)−Pt(1)−C(1)	83.7(3)	Mo(1)−Pt(1)−N(1)	103.2(2)
C(1)−Pt(1)−P(1)	90.2(3)	N(1)−Pt(1)−P(1)	82.8(2)
Mo(1)−C(25)−O(1)	162.6(9)	Mo(1)−C(26)−O(2)	167.1(7)
Mo(1)−C(27)−O(3)	175(1)	Pt(1)−Mo(1)−C(25)	54.0(3)
Pt(1)−Mo(1)−C(26)	58.2(2)	Pt(1)−Mo(1)−C(27)	102.8(3)

ML_n rather than Me, with a strong trans influence in solution.[4] The trans influence of Co is smaller than that of Mo and W (see Experimental Section). In the ^{1}H NMR spectra, the methylene protons of the NCH_2CH_3 moiety for **5** and **6** are diastereotopic, suggesting rigid coordination of the nitrogen atom to the Pt center. In contrast, the methylene protons of **1**−**4** appeared as a quartet or a broad singlet, suggesting involvement of some dynamic processes (vide infra). Methylene signals of the PCH_2CH_2N unit of **2** appear as a broad doublet and singlet at δ 2.7 and 2.8 due to coupling with a neighboring P nucleus at 258 K. The peak of the lower field in the doublet accidentally overlaps with the singlet, giving two apparently broad singlets in a 1:3 ratio.

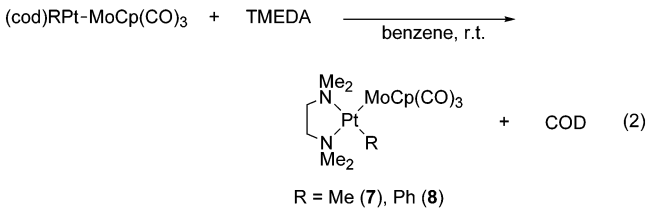

Heterodinuclear organoplatinum complexes with a bidentate nitrogen ligand, (tmeda-κ^2N,N')RPt−$MoCp(CO)_3$ [R = Me (**7**), Ph (**8**)], have also been synthesized by the ligand exchange reaction of (cod)RPt−$MoCp(CO)_3$ with TMEDA (eq 2). ^{1}H NMR of **7** and **8** show two sharp methyl resonances for TMEDA with Pt satellites, indicating square-planar geometry at Pt with rigid coordination of TMEDA.

Dynamic Behavior of the PN Chelate Ligand. Variable-temperature (VT) ^{1}H NMR of **2** and **4** show dynamic behavior for the diastereotopic methylene protons of the coordinating diethylamino moiety, while other signals remain sharp. The methylene protons of the ethyl group in **2** or **4** appear as a broad singlet or quartet at room temperature. However, on lowering the temperature as shown in Figure 2, the signal initially broadens and then gradually splits into two peaks. At

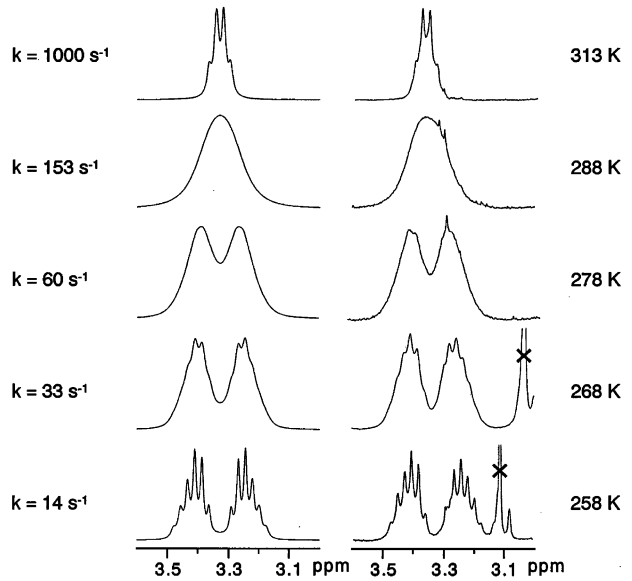

Figure 2. Variable-temperature ^{1}H NMR spectra of the diastereotopic methylene protons in the NEt_2 moiety of **2** in CD_3COCD_3. (right) Observed spectra. (left) Simulated spectra. × indicates impurity.

258 K, two doublets of quartets with equal intensity appear due to couplings between the diastereotopic geminal protons, which further couple to the methyl protons.

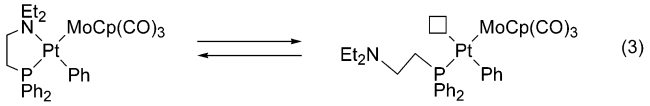

(3)

On the other hand, Cp resonanes in ^{1}H NMR spectra of **2** or **4** show no notable change in this temperature range. This dynamic behavior is conveniently interpreted by the facile and reversible Pt−N bond rupture, making the two diastereotopic methylene protons magnetically equivalent (eq 3). Such hemilabile behavior had been reported for some mononuclear platinum or palladium complexes with PN[11] or bidentate nitrogen ligands.[12] From the line shape analysis of these VT NMR spectra of **2**, dissociation rate constants of the amino group at various temperatures were estimated in both acetone and toluene, giving kinetic parameters as follows: $\Delta G_{273}^{\ddagger} = 57.9$ kJ mol^{-1}, $\Delta H^{\ddagger} = 49.8$ kJ mol^{-1}, $\Delta S^{\ddagger} = -29.7$ J mol^{-1} K^{-1} in CD_3COCD_3 and $\Delta G_{273}^{\ddagger} = 56.4$ kJ mol^{-1}, $\Delta H^{\ddagger} = 63.0$ kJ mol^{-1}, $\Delta S^{\ddagger} = 24.2$ J mol^{-1} K^{-1} in $C_6D_5CD_3$. It is interesting to note that the $\Delta S^{\ddagger}$ value obtained in CD_3COCD_3 is negative, but positive in $C_6D_5CD_3$, despite the dissociative nature of the reaction. The fact suggests that the coordination of CD_3COCD_3 to the Pt center is involved in stabilizing the resulting unstable three-coordinate species in CD_3COCD_3, whereas in $C_6D_5CD_3$ it does not coordinate or very weakly coordinates to Pt. Despite this difference, the observed $\Delta G_{273}^{\ddagger}$ values are very close to each other, showing their good compensation effect of $\Delta H^{\ddagger}$ and $\Delta S^{\ddagger}$ in this reaction.

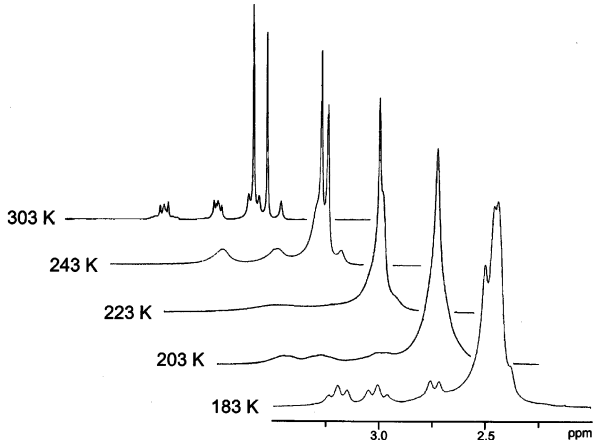

Figure 3. Variable-temperature ^{1}H NMR spectra of the methyl and methylene regions in coordinating TMEDA of **8** in CD_2Cl_2.

On the other hand, the methylene resonance of **1** started to broaden at 233 K, but did not reach the coalescence point even lowering to 180 K. The difference of the dissociation rates in **1** and **2** may be attributable to the difference of the trans effect of Me and Ph ligands; the rate of Pt−N bond rupture trans to Me in **1** is much faster than that trans to Ph in **2**.

In contrast, the methylene protons of the ethyl group in Pt−Co complexes **5** and **6** appear as two well-separated doublets of quartets (**5**: δ 2.93 and 3.23, **6**: δ 3.01 and 3.28 in $C_6D_5CD_3$) at ambient temperature, indicating no such dynamic behavior. However, on raising the temperature to 373 K in $C_6D_5CD_3$, these signals gradually broadened but did not reach complete coalescence. Kinetic parameters are also estimated from these limited data as follows: $\Delta G_{273}^{\ddagger} = 74.2$ kJ mol^{-1}, $\Delta H^{\ddagger} = 78.5$ kJ mol^{-1}, $\Delta S^{\ddagger} = 15.4$ J mol^{-1} K^{-1} for **5** and $\Delta G_{273}^{\ddagger} = 76.8$ kJ mol^{-1}, $\Delta H^{\ddagger} = 84.5$ kJ mol^{-1}, $\Delta S^{\ddagger} = 28.3$ J mol^{-1} K^{-1} for **6**.

The large $\Delta G^{\ddagger}$ values for Pt−Co complexes compared to Pt−Mo complexes imply that the Pt−N bond rupture for Pt−Co complexes is more difficult than that for Pt−Mo complexes. This may be due to a decrease in electron density at Pt, making coordination of the nitrogen donor to Pt stronger, since the Mo anion is a better donor than Co. Although the difference of the estimated $\Delta G^{\ddagger}$ values for **5** and **6** is small, it is an indication of trans effect of the Me and Ph ligands.

In the case of Pt−Mo analogues having a symmetrical bidentate phosphine ligand, (dppe-κ^2P,P')MePt−MoCp-$(CO)_3$,[4c] such a dynamic process was not observed and the DPPE ligand rigidly binds to the Pt center in a bidentate fashion even at 70 °C. On the other hand, the Pt−Mo complex with TMEDA (**8**) in CD_2Cl_2 shows dynamic behavior in its VT ^{1}H NMR spectra (Figure 3), though TMEDA is not unsymmetrical.

The proton NMR resonances of the methylene protons of TMEDA are observed as two inequivalent multiplets at δ 2.74 and 2.98 at ambient temperature, due to different trans ligands of Me and Mo. At temperature below 263 K, the resonances begin to broaden and

(10) (a) Piper, T. S.; Wilkinson, G. *J. Inorg. Nucl. Chem.* **1956**, *3*, 104. (b) Burlitch, J. M.; Theyson, T. W. *J. Chem. Soc., Dalton Trans.* **1974**, 828.

(11) (a) la Torre, F. G.; Jalón, F. A.; López-Agenjo, A.; Manzano, B. R.; Rodríguez, A.; Strum, T.; Weissensteiner, W.; Martínez-Ripoll, M. *Organometallics* **1988**, *7*, 4634. (b) Amatore, C.; Fuxa, A.; Jutand, A. *Chem. Eur. J.* **2000**, *6*, 1474.

(12) (a) Romeo, R.; Scolaro, L. M.; Nastasi, N.; Arena, G. *Inorg. Chem.* **1996**, *35*, 5087. (b) Delis, J. G. P.; Aubel, P. G.; Vrieze, K.; van Leeuwen, P. W. N. M.; Veldman, N.; Spek, A. L.; van Neer, F. J. R. *Organometallics* **1997**, *16*, 2948. (c) Gogoll, A.; Örnebro, J.; Grennberg, H.; Bäckvall, J. E. *J. Am. Chem. Soc.* **1994**, *116*, 3631.

Scheme 2

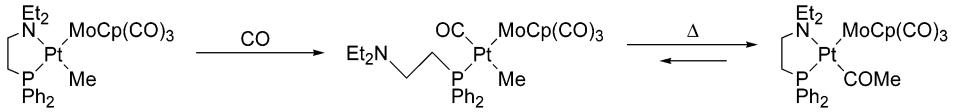

1 **9** **14**

decoalesce at 213 K. On further lowering the temperature, two sets of signals gradually appeared at 183 K, each set consisting of a triplet and a doublet, probably due to selective couplings between geminal and vicinal protons, although one doublet signal at higher field is obscured by overlapping with large methyl signals of TMEDA. One of the couplings between two vicinal protons may be negligible due to a coincidental H−C−C−H dihedral angle of 90° by the restricted ligand conformation. It is also notable that the dynamic process is independent of addition of free TMEDA. This observation indicates that this dynamic process does not involve dissociation of the nitrogen atom from the Pt center, but an intramolecular process. Therefore for the present dynamic behavior, a mechanism involving a facile equatorial/axial hydrogen site exchange process due to interconversion between the λ and δ conformers is proposed (eq 4).[13]

(4)

δ λ

As described earlier, the facile intramolecular dissociation process of the N atom in the PN ligand of **2** is frozen out in the ^{1}H NMR at 258 K. However, further lowering of the temperature to 213 K caused another line broadening of both methylene signals of the ethyl and PC_2H_4N units. The dynamic behavior may also be originated from the fast conformation change of the methylene chain, although observation of the complete rigid structure is not successful under the observed temperature.

Reaction of Heterodinuclear Complexes with CO. When **1**−**4** were treated with CO (1 atm) in acetone or benzene, the coordinating nitrogen atom of the PN ligand was readily displaced by CO to give ($Et_2NC_2H_4PPh_2$-κ^1P)(CO)RPt−$MCp(CO)_3$ (**9**−**12**) (eq 5).

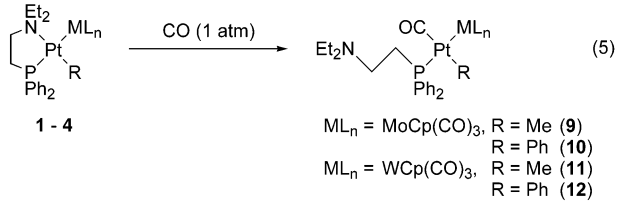

(5)

1 - 4

ML_n = $MoCp(CO)_3$, R = Me (**9**)
R = Ph (**10**)
ML_n = $WCp(CO)_3$, R = Me (**11**)
R = Ph (**12**)

In the ^{1}H NMR of **9**, the chemical shift of the methylene group of the NCH_2CH_3 moiety was observed to be very close to that of free $Et_2NC_2H_4PPh_2$. The methyl group attached to Pt appeared as a singlet with ^{195}Pt satellites, the $^2J_{Pt-H}$ coupling constant value being 61 Hz for **9**, which is smaller than that for **1** (74 Hz). The difference reflects a stronger trans influence of the CO ligand than the nitrogen ligand. In the $^{13}C\{^1H\}$ NMR spectroscopy of **9**, one of the carbonyl carbons appeared as a singlet at δ 189.2 ($^1J_{Pt-C}$ = 1031 Hz) with ^{195}Pt satellites. The $^1J_{Pt-C}$ value is comparable to the coupling constant of 906 Hz in $PtPhCl(CO)(PMePh_2)$, where CO is located cis to the phosphorus atom and trans to the Ph group.[14] The IR spectrum of **9** shows a strong ν(CO) band at 2039 cm^{-1}. The molar electric conductivity of **9** in THF was very low, suggesting that **9** is not an ionic complex but a neutral one. From these results, the N atom is not coordinated to Pt as shown in eq 5, and CO is located at the site cis to P and trans to the methyl group. However, the symmetrical bidentate phosphine analogue (dppe-κ^2P,P')MePt−$MoCp(CO)_3$[4c] did not react at all with CO under the same reaction conditions. On the other hand, the reaction of the Pt−Mo dinuclear complex **7** having a TMEDA ligand with CO (1 atm) in CD_3COCD_3 did not cause a partial displacement of the NMe_2 group by CO, but resulted in formation of the cationic complex [PtMe(CO)(tmeda-κ^2N,N')]$^+$[$MoCp(CO)_3$]$^-$ (**13**) with a small amount of uncharacterized "Pt−Me" species [δ 0.96, $^2J_{Pt-H}$ = 62.8 Hz]. The "Pt−Me" species is tentatively assigned as [$PtMe(CO)_3$]$^+$[$MoCp(CO)_3$]$^-$, since complete liberation of TMEDA was followed. However, addition of 2 equiv of TMEDA completely suppressed the formation of the "Pt−Me" species and formation of only **13** was observed. In the ^{1}H NMR of **13**, the chemical shift of the Cp resonance was identical to anionic complex Na[$MoCp(CO)_3$]. Two methyl resonances for TMEDA are observed at δ 2.94 and 3.24 with ^{195}Pt satellites ($^3J_{Pt-H}$ = 39.4 and 22.8 Hz, respectively), and the Pt-Me signal appears at δ 0.90 with a $^2J_{Pt-H}$ of 69.1 Hz. These observations indicate that the resulting cationic complex has a square-planar geometry, as depicted in eq 6. Preferential formation of the cationic complex may possibly be due to stabilization of the cationic complex with TMEDA by its strong electron donation.

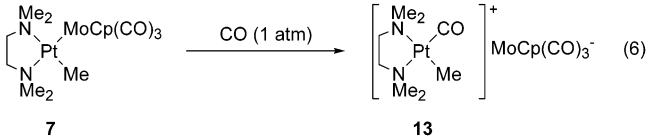

(6)

7 **13**

Heating of the carbonyl complex **9** in C_6D_6 at 70 °C for 1 day caused insertion of CO into the Pt−Me bond, giving the acetyl complex ($Et_2NC_2H_4PPh_2$-κ^2N,P)(MeCO)Pt−$MoCp(CO)_3$ (**14**) as an equilibrium mixture with **9** in a 3:2 ratio (Scheme 2). Further heating of the mixture did not change the molar ratio but caused only some decomposition. On the other hand, heating of the

(13) (a) de Graaf, W.; Boersma, J.; Smeets, W. J. J.; Spek, A. L.; van Koten, G. *Organometallics* **1989**, *8*, 2907. (b) Hughes, R. P.; Overby, J. S.; Williamson, A.; Lam, K.; Concolino, T. E.; Rheingold, A. L. *Organometallics* **2000**, *19*, 5190.

(14) (a) Anderson, G. K.; Cross, R. J. *Acc. Chem. Res.* **1984**, *17*, 67. (b) Anderson, G. K.; Cross, R. *J. Chem. Soc., Dalton Trans.* **1979**, 1246.

Scheme 3

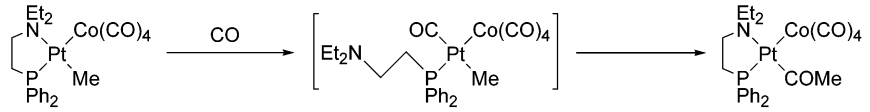

5 **16** **15**

independently prepared acetyl complex **14** from Pt(COMe)Cl($Et_2NC_2H_4PPh_2$-κ^2N,P) and Na[$MoCp(CO)_3$] at 70 °C in C_6D_6 for 1 day also gave the same mixture of **9** and **14** in the same ratio. This indicates that the slow equilibration of this reversible CO insertion is taking place at 70 °C.

On the other hand, reaction of the Pt−Co complex having a PN ligand **5** with CO gave only the acetyl complex **15**. However, monitoring the reaction of **5** with CO by ^1H and $^{31}P\{^1H\}$ NMR spectroscopy in C_6D_6 at 30 °C revealed the initial formation of the carbonyl complex **16** followed by slow formation of **15**, indicating a successive reaction mechanism (Scheme 3). The CO insertion reaction of **5** was significantly faster than that of the DPPE analogue (dppe-κ^2P,P')MePt−$Co(CO)_4$.[4e,i] When **5** was treated with 1 atm of CO in C_6D_6 at 30 °C for 24 h, the corresponding acetyl complex **15** was obtained quantitatively, whereas the reaction of (dppe-κ^2P,P')MePt−$Co(CO)_4$ with CO under the same conditions gave the corresponding acetyl complex (dppe-κ^2P,P')(MeCO)Pt−$Co(CO)_4$ in only 26% yield. The following two mechanisms are proposed for this CO insertion from **16**: (i) Methyl migration from Pt to Co initially takes place, followed by fast CO insertion into the Co−Me bond, and then migration of the resulting acetyl group at Co to Pt as previously reported in CO insertion into the Me-Pd−Co complex.[4i] (ii) Initial ionization takes place by heterolytic cleavage of the Pt−Co bond, and then CO coordinates to Pt cis to the Me group, leading to facile insertion. Other mechanisms, including a five-coordinate intermediate as reported in mononuclear Pt or Pd complexes or direct initial isomerization from trans to cis followed by insertion, are also possible as reaction pathways.[5c,14a,15]

Reaction of 1 with Tertiary Phosphine Ligands. When **1** was treated with various tertiary phosphines (PR_3 = $Et_2NC_2H_4PPh_2$, PMe_3, PEt_3, PPh_3, $P(OMe)_3$), heterolytic cleavage of the metal−metal bond took place to give ionic complexes **17**−**21** (eq 7).

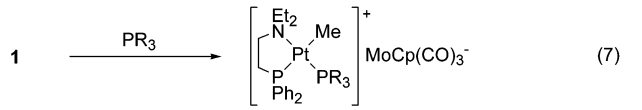

(7)

PR_3 = $Et_2NC_2H_4PPh_2$ (**17**), PMe_3 (**18**), PEt_3 (**19**), PPh_3 (**20**), $P(OMe)_3$ (**21**)

Such ionization reactions are frequently observed in the reactions of square-planar d^8 transition metal complexes and heterodinuclear complexes with tertiary phosphines.[4b,d,16,17] It is interesting to note that reaction of (cod)MePt−$MoCp(CO)_3$ with a stoichiometric amount of $Et_2NCH_2H_4PPh_2$ caused selective ioinization to give **17** in 50% yield and half of the starting complex remained intact. This fact prevented us from using the ligand displacement method for the preparation of heterodinuclear complexes with a PN ligand. Occurrence of preferential ionization of the Pt−Mo bond rather than ligand displacement on interaction of heterodinuclear complexes with tertiary phosphine ligands is of interest. This could be due to effective stabilization of cationic platinum(II) species by coordination of phosphines, although a more detailed investigation is needed for a complete understanding of this reaction selectivity.

Single crystals of complex **21** suitable for X-ray structure analysis were obtained by recrystallization from THF/ether. The crystal data, selected bond lengths and distances, and an ORTEP drawing are shown in Tables 1 and 3 and Figure 4, respectively.

The geometry around Pt is square planar, in which two P atoms coordinate to Pt in a cis fashion. The Mo moiety has a three-leg piano-stool geometry. Three Mo−C−O angles are almost linear and the Pt−Mo distance is 6.54 Å, indicating no M−M bond. The result is consistent with the ionic structure involving the Pt cation and Mo anion. ^1H NMR of **17**−**21** shows two diasteteotopic methylene protons of NCH_2CH_3 at δ 3.3−

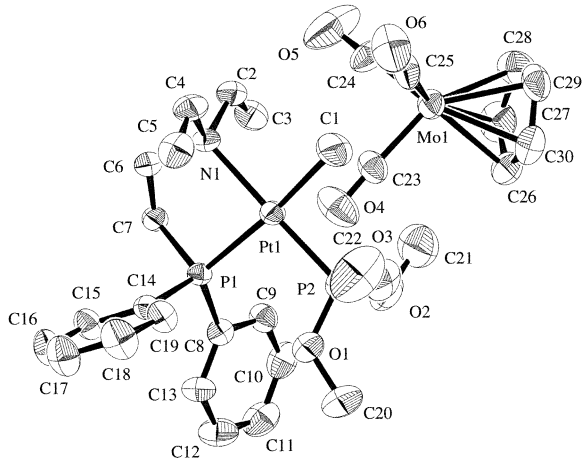

Figure 4. ORTEP drawing of [PtMe{$P(OMe)_3$}($Et_2NC_2H_4PPh_2$-κ^2N,P)]$^+$[$MoCp(CO)_3$]$^-$ (**21**). All hydrogen atoms are omitted for clarity. Ellipsoids represent 50% probability.

Table 3. Selected Bond Lengths and Angles for 21

Bond Lengths (Å)			
Pt(1)−P(1)	2.306(1)	Pt(1)−P(2)	2.175(1)
Pt(1)−N(1)	2.212(4)	Pt(1)−C(1)	2.091(6)
Mo(1)−C(23)	1.919(5)	Mo(1)−C(24)	1.936(6)
Mo(1)−C(25)	1.912(5)	Mo(1)−C(26)	2.381(5)
Mo(1)−C(27)	2.369(6)	Mo(1)−C(28)	2.377(7)
Mo(1)−C(29)	2.379(6)	Mo(1)−C(30)	2.390(6)
O(4)−C(23)	1.178(7)	O(5)−C(24)	1.150(8)
O(6)−C(25)	1.205(7)		

Bond Angles (deg)			
P(1)−Pt(1)−P(2)	95.90(5)	P(1)−Pt(1)−N(1)	84.1(1)
P(2)−Pt(1)−C(1)	89.4(2)	N(1)−Pt(1)−C(1)	90.6(2)
C(23)−Mo(1)−C(24)	88.2(3)	C(23)−Mo(1)−C(25)	89.5(2)
C(24)−Mo(1)−C(25)	86.1(3)	Mo(1)−C(23)−O(4)	178.1(5)
Mo(1)−C(24)−O(5)	178.2(7)	Mo(1)−C(25)−O(6)	178.2(6)

(15) Garrou, P. E.; Heck, R. F. *J. Am. Chem. Soc.* **1976**, *98*, 4115.
(16) (a) Clark, H. C.; Ruddick, J. D. *Inorg. Chem.* **1970**, *9*, 1226. (b) Hooton, K. A. *J. Chem. Soc. A* **1970**, 1896. (c) Komiya, S.; Kochi, J. K. *J. Am. Chem. Soc.* **1976**, *98*, 7599.

Scheme 4

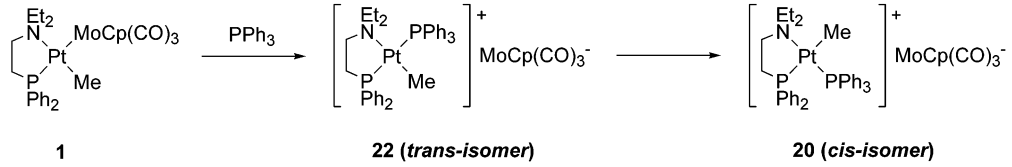

1 **22** (*trans-isomer*) **20** (*cis-isomer*)

3.7, indicating rigid bidentate coordination of the PN ligand to the electron-deficient cationic Pt center. The Pt-Me group appears as a doublet of doublets with ^{195}Pt satellites, indicating the existence of two magnetically inequivalent cis phosphorus nuclei at Pt. Consistently, the ^{31}P{^{1}H} NMR shows two doublets with a small cis coupling constant ($^2J_{P-P}$ = 12 Hz) having ^{195}Pt satellites, the value being similar to that reported for *cis*-PtPhCl(PMe$_3$)$_2$ (14.6 Hz).[18a] The molar electric conductivity of one of these complexes, **17**, is found to be very large (Λ = 12.6 S cm^2 mol^{-1}), supporting its ionic structure.

To reveal the reaction path of the formation of the cis product, time courses of the reaction of **1** were followed by ^{1}H NMR spectroscopy in CD_3COCD_3 at 50 °C. Immediately after addition of 1 equiv of PPh_3, ionization took place, but the product was only the trans isomer **22**. Then the cis product **20** was slowly formed as shown in Scheme 4.

^{31}P{^{1}H} NMR of the trans isomer **22** showed two doublets with ^{195}Pt satellites. The observed large $^2J_{P-P}$ value of 405 Hz is consistent with the trans configuration of the two P nuclei and is comparable to that reported for [PtMe(PPh$_3$)(dppe)]$^+$I$^-$ ($^2J_{P-P}$ = 381.4 Hz).[18b] In the ^{1}H NMR, the methyl group on Pt is observed as a doublet of doublets ($^3J_{P-H}$ = 8.1, 6.6 Hz) with a ^{195}Pt satellite. The chemical shift of the Cp resonance of the trans isomer (**22**) was identical to that of the cis isomer (**20**). When 5 equiv of PPh_3 was added to the solution of **1**, the cis−trans isomerization rate was significantly accelerated, though the ionization process was not affected at all (Figure 5). The results suggest that the trans−cis isomerization process involves a prior association step of the phosphorus ligand to **22**, giving a five-coordinate intermediate.

From these observations, the reaction of **1** with a tertiary phosphine ligand is considered to proceed by a facile initial heterolytic M−M′ bond cleavage by coordination of the phosphine ligand to give the trans isomer **22**. Then the trans isomer **22** slowly isomerizes to the cis isomer **20** by an associative process.

It is interesting to note that the reaction of (dppe-κ^2P,P')MePt−MoCp(CO)$_3$ with PPh_3 also caused heterolytic M−M′ bond cleavage to give [PtMe(PPh$_3$)(dppe-κ^2P,P')]$^+$[MoCp(CO)$_3$]$^-$ (**23**).[4d] On the other hand, the reaction of the TMEDA analogue **7** with 3 equiv of PPh_3 in CD_3COCD_3 gave a mixture of two ionic complexes, [PtMe(PPh$_3$)(tmeda)]$^+$[MoCp(CO)$_3$]$^-$ (**24**) and [PtMe(PPh$_3$)$_3$]$^+$[MoCp(CO)$_3$]$^-$ (**25**), in 12% and 88% yield, respectively. Upon addition of excess PPh_3 to the mixture and heating of the solution at 50 °C for a day, **24** was completely converted into **25**, though a neutral intermediate complex having a κ^1-coordinated TMEDA ligand was not detected.

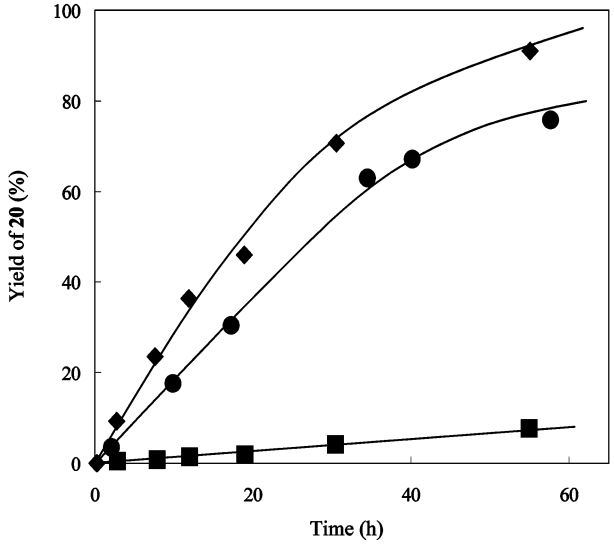

Figure 5. Time−yield curves for trans−cis isomerization from **22** to **20**. Conditions: temp = 30 °C, [**22**] = 1.5 × 10^{-2} M, solvent = CD_3COCD_3. [PPh$_3$]/[**22**] = 0 (■), 2 (●), 4 (◆).

Summary

In the present study, synthesis of a series of novel heterodinuclear organoplatinum complexes having an unsymmetrical PN ligand (2-(diphenylphosphino)triethylamine) or bidentate nitrogen ligand (*N*,*N*,*N*′,*N*′-tetramethylethylenediamine) is described. Dynamic behavior arising from a facile reversible Pt−N bond rupture was observed for complexes with a PN ligand. This hemilabile nature of the PN ligand leads to the high reactivity of (Et$_2$NC$_2$H$_4$PPh$_2$-κ^2N,P)RPt−MCp(CO)$_3$ **1**−**4** toward CO to give (Et$_2$NC$_2$H$_4$PPh$_2$-κ^1P)(CO)RPt−MCp(CO)$_3$ **9**−**12** having a monodentate phosphorus coordination. It is interesting to note that reaction of dinuclear complexes **1**−**4** having hemilabile PN ligands with CO caused substitution of the N ligand, whereas interaction with phosphorus ligands induced heterolytic cleavage of the Pt−Mo bond, giving ionic complexes. This could be due to the strong back-bonding property of CO on coordination of the stabilizing neutral complex (Et$_2$NC$_2$H$_4$PPh$_2$-κ^1P)(CO)RPt−MoCp(CO)$_3$. In contrast, strong electron donation to Pt by the phosphorus ligand may favor an electron-deficient cationic Pt center rather than the possible neutral complex as above. Facile CO insertion was observed for the Pt−Co complex having a PN ligand. The reaction could involve a similar mechanism of a facile CO insertion process of (dppe-κ^2P,P')MeM−Co(CO)$_4$ (M = Pd, Pt),[4e,i] where an initial alkyl migration from Pd (or Pt) to Co followed by insertion of CO at Co and oxidative addition of acetyl-

(17) (a) Bearman, P. S.; Smith, A. K.; Tong, N. C.; Whyman, R. *Chem. Commun*. **1996**, 2061. (b) Schubart, M.; Mitchell, G.; Gade, L. H.; Scowen, I. J.; McPartlin, M. *Chem. Commun*. **1999**, 223. (c) Roberts, D. A.; Mercer, W. C.; Geoffroy, G. L.; Pierpont, C. G. *Inorg. Chem*. **1986**, *25*, 1439.

(18) (a) Kayaki, Y.; Tsukamoto, H.; Kaneko, M.; Shimizu, I.; Yamamoto, A.; Tachikawa, M.; Nakajima, T. *J. Organomet. Chem*. **2001**, *622*, 199. (b) You, Y. J.; Chem. J. T.; Cheng, M. C.; Wang, Y. *Inorg. Chem*. **1991**, *30*, 3621.

cobalt species to Pd (or Pt) gives the insertion product. Ligand transfer of the CO ligand from Pt or Co and recoordination of the N atom of the PN ligand should also be involved in this process, although a further detailed investigation is required. Introduction of the hemilabile PN ligand would provide a highly reactive specific reaction site not only in the heterodinuclear complex but also in various transition metal complexes.

Experimental Section

All manipulations were carried out under a dry nitrogen or argon atmosphere using standard Schlenk and vacuum line techniques. Solvents were refluxed over and distilled from appropriate drying agents under N_2: benzene, toluene, hexane, THF, and Et_2O from sodium benzophenone ketyl; acetone from Drierite; CH_2Cl_2 from P_2O_5. Deuterated solvents were degassed by three freeze−pump−thaw cycles and then vacuum transferred from appropriate drying agents (C_6D_6 and $C_6D_5CD_3$ from sodium wire; $CDCl_3$ and CD_2Cl_2 from P_2O_5, CD_3COCD_3 from Drierite). PtMeCl(cod),[19] PtPhCl(cod),[19] Na[MoCp(CO)$_3$],[10] Na[WCp(CO)$_3$],[10] Na[Co(CO)$_4$],[20] and $Et_2NC_2H_4PPh_2$[21] were prepared according to literature procedures. NMR spectra were recorded on a JEOL LA-300 spectrometer (300.4 MHz for ^{1}H, 121.6 MHz for ^{31}P, and 75.5 MHz for ^{13}C) with chemical shifts reported in ppm downfield from TMS for ^{1}H and ^{13}C and from 85% H_3PO_4 in D_2O. IR spectra were recorded on a JASCO FT/IR-410 spectrometer using KBr disks. Elemental analyses were carried out with a Perkin-Elmer 2400 series II CHN analyzer. Molar electrical conductivity was measured on a TOA Conduct Meter CM 7B.

PtMeCl($Et_2NC_2H_4PPh_2$-κ^2*N,P*). 2-(Diphenylphosphino)-triethylamine $Et_2NC_2H_4PPh_2$ (0.63 mL, 3.0 mmol) was added to a benzene solution of PtMeCl(cod) (1.049 g, 2.972 mmol). After the mixture was stirred for 1 h at room temperature, the resulting white-yellow precipitate was filtered and washed with hexane. The product was recrystallized from CH_2Cl_2 at −30 °C to give light yellow crystals of PtMeCl($Et_2NC_2H_4PPh_2$-κ^2*N,P*). Yield: 76% (1.21 g, 2.28 mmol). Anal. Calcd for $C_{19}H_{27}ClNPPt$: C, 42.98; H, 5.13; N, 2.64. Found: C, 42.57; H, 5.01; N, 2.66. ^{1}H NMR ($CDCl_3$): δ 0.58 (3H, d, $^3J_{P-H}$ = 4.2 Hz, $^2J_{Pt-H}$ = 76.0 Hz, Pt-Me), 1.25 (6H, t, $^3J_{H-H}$ = 7.0 Hz, Me (N-Et)), 2.4−2.8 (4H, m, C*H*$_2$-C*H*$_2$), 3.14 (2H, dq, $^2J_{H-H}$ = 12.9 Hz, $^3J_{H-H}$ = 7.0 Hz, C*H*$_2$ (N-Et)), 3.40 (2H, dq, $^2J_{H-H}$ = 12.9 Hz, $^3J_{H-H}$ = 7.0 Hz, C*H*$_2$ (N-Et)), 7.4−7.6 (10H, m, Ph). ^{31}P{^{1}H} NMR ($CDCl_3$): δ 27.4 (s, $^1J_{Pt-P}$ = 4862 Hz).

PtPhCl($Et_2NC_2H_4PPh_2$-κ^2*N,P*). The same procedure was used as described for PtMeCl($Et_2NC_2H_4PPh_2$-κ^2*N,P*). Reaction of PtPhCl(cod) (578.2 mg, 1.391 mmol) with $Et_2NC_2H_4PPh_2$ (0.300 mL, 1.41 mmol) gave 483.3 mg (0.8150 mmol, 59%) of PtPhCl($Et_2NC_2H_4PPh_2$-κ^2*N,P*). Anal. Calcd for $C_{24}H_{29}ClNPPt$: C, 48.61; H, 4.93; N, 2.36. Found: C, 48.50; H, 4.79; N, 2.24. ^{1}H NMR ($CDCl_3$): δ 1.36 (6H, t, $^3J_{H-H}$ = 7.0 Hz, Me (N-Et)), 2.40−2.75 (4H, m, C*H*$_2$-C*H*$_2$), 3.20 (4H, dq, $^2J_{H-H}$ = 13.0 Hz, $^3J_{H-H}$ = 7.0 Hz, C*H*$_2$ (N-Et)), 3.46 (4H, dq, $^2J_{H-H}$ = 13.0 Hz, $^3J_{H-H}$ = 7.0 Hz, C*H*$_2$ (N-Et)), 6.65−6.69 (3H, m, *m*- and *p*-Ph (Pt-Ph)), 6.98 (2H, m, $^3J_{Pt-H}$ = 46.0 Hz, *o*-Ph (Pt-Ph)), 7.30−7.55 (10H, m, Ph). ^{31}P{^{1}H} NMR ($CDCl_3$): δ 23.3 (s, $^1J_{Pt-P}$ = 4774 Hz).

Pt(COMe)Cl($Et_2NC_2H_2PPh_2$-κ^2*N,P*). PtMeCl($Et_2NC_2H_4PPh_2$-κ^2*N,P*) (119.5 mg, 0.2251 mmol) was dissolved in CH_2Cl_2, and the solution was evacuated. Carbon monoxide (0.1 MPa) was then introduced. After stirring the solution for 5 days, the dark green reaction mixture was treated with activated charcoal and filtered to give a pale yellow solution. The solution was concentrated under reduced pressure and recrystallized from a mixture of CH_2Cl_2/hexane. Yield: 65% (82.0 mg, 0.147 mmol). Anal. Calcd for $C_{20}H_{27}ClNOPPt$: C, 42.98; H, 4.87; N, 2.51. Found: C, 42.84; H, 4.84; N, 2.46. ^{1}H NMR (C_6D_6): δ 1.27 (6H, t, $^3J_{H-H}$ = 6.9 Hz, Me (N-Et)), 1.96 (3H, s, Pt-COMe), 2.4−2.7 (4H, m, C*H*$_2$-C*H*$_2$), 3.03 (2H, dq, $^2J_{H-H}$ = 13.0 Hz, $^3J_{H-H}$ = 6.9 Hz, C*H*$_2$ (N-Et)), 3.25 (2H, dq, $^2J_{H-H}$ = 13.0 Hz, $^3J_{H-H}$ = 6.9 Hz, C*H*$_2$ (N-Et)), 7.5 (6H, m, *m*- and *p*-Ph), 7.7 (4H, m, *o*-Ph). ^{31}P{^{1}H} NMR (C_6D_6): δ 10.2 (s, $^1J_{Pt-P}$ = 5031 Hz). IR (KBr, cm^{-1}): 715(m), 1099(m), 1435(m), 1634(s).

($Et_2NC_2H_4PPh_2$-κ^2N,P)MePt−MoCp(CO)$_3$ (1). PtMeCl($Et_2NC_2H_4PPh_2$-κ^2*N,P*) (211 mg, 0.398 mmol) and $AgNO_3$ (90 mg, 0.52 mmol) were dissolved in THF, and the suspension was stirred for one night at room temperature to give a pale yellow solution with a white precipitate of AgCl. The precipitate was filtered off, and the resulting solution was added dropwise to a THF solution of Na[MoCp(CO)$_3$] (161 mg, 0.598 mmol) under −70 °C. Then the mixture was stirred for 3 h at −30 °C. All volatile matters were removed by evaporation, and the resulting brown-yellow solid was extracted with toluene at −20 °C. After the filtered solution was concentrated under reduced pressure at −20 °C, excess hexane was added to give an analytically pure yellow powder. The product was filtered, washed with hexane, and dried under vacuum at room temperature. Yield: 87% (258 mg, 0.348 mmol). Anal. Calcd for $C_{27}H_{32}MoNO_3PPt$: C, 43.79; H, 4.36; N, 1.89. Found: C, 43.88; H, 4.36; N, 1.81. Molar electric conductivity Λ (THF, 20 °C): 0.9 S cm^2 mol^{-1}. ^{1}H NMR (CD_3COCD_3): δ 0.38 (3H, d, $^3J_{P-H}$ = 5.4 Hz, $^2J_{Pt-H}$ = 74 Hz, Pt-Me), 1.18 (6H, t, $^3J_{H-H}$ = 7.0 Hz, Me (N-Et)), 2.2−2.8 (4H, m, C*H*$_2$-C*H*$_2$), 3.4 (4H, q, $^3J_{H-H}$ = 6.9 Hz, C*H*$_2$ (N-Et)), 5.24 (5H, s, Cp), 7.50−7.60 (6H, m, *m*- and *p*-Ph), 7.84−7.94 (4H, m, *o*-Ph). ^{31}P{^{1}H} NMR (CD_3COCD_3): δ 40.3 (s, $^1J_{Pt-P}$ = 4208 Hz). IR (KBr, cm^{-1}): 503(m), 1102(m), 1435(m), 1761(vs), 1788(vs), 1879(s).

The following heterodinuclear complexes **2**−**6** were prepared analogously as described for **1**.

($Et_2NC_2H_4PPh_2$-κ^2*N,P*)PhPt−MoCp(CO)$_3$ (2). A pale orange powder was formed. Yield: 77%. Anal. Calcd for $C_{32}H_{34}MoNO_3PPt$: C, 47.89; H, 4.27; N, 1.75. Found: C, 47.52; H, 4.50; N, 1.50. ^{1}H NMR (CD_3COCD_3): δ 1.21 (6H, t, $^3J_{H-H}$ = 7.2 Hz, Me (N-Et)), 2.7−2.9 (4H, m, C*H*$_2$-C*H*$_2$), 3.4 (4H, brs, C*H*$_2$ (N-Et)), 5.20 (5H, s, Cp), 6.4−6.5 (3H, m, *m*- and *p*-Ph (Pt−Ph)), 6.93 (2H, m, $^3J_{H-H}$ = 8.4 Hz, $^4J_{H-H}$ = 1.5 Hz, $^3J_{Pt-H}$ = 56 Hz, *o*-Ph (Pt−Ph)), 7.3−7.6 (10H, m, Ph). ^{31}P{^{1}H} NMR (CD_3COCD_3): δ 34.4 (s, $^1J_{Pt-P}$ = 4087 Hz). IR (KBr, cm^{-1}): 739(m), 1434(m), 1792(vs), 1891(s).

($Et_2NC_2H_4PPh_2$-κ^2*N,P*)MePt−WCp(CO)$_3$ (3). Na[WCp(CO)$_3$] was used instead of Na[MoCp(CO)$_3$]. Yellow powder. Yield: 87%. Anal. Calcd for $C_{27}H_{32}NO_3PPtW$: C, 43.16; H, 3.85; N, 1.57. Found: C, 43.19; H, 4.18; N, 1.42. ^{1}H NMR (C_6D_6): δ 0.88 (6H, t, $^3J_{H-H}$ = 7.2 Hz, Me (N-Et)), 0.98 (3H, d, $^3J_{P-H}$ = 6.3 Hz, $^2J_{Pt-H}$ = 79 Hz, Pt-Me), 1.8−2.1 (4H, m, C*H*$_2$-C*H*$_2$), 3.29 (4H, q, $^3J_{H-H}$ = 7.2 Hz, C*H*$_2$ (N-Et)), 5.05 (5H, s, Cp), 7.0−7.16 (6H, m, *m*- and *p*-Ph), 7.75−7.83 (4H, m, *o*-Ph). ^{31}P{^{1}H} NMR (C_6D_6): δ 41.9 (s, $^1J_{Pt-P}$ = 4149 Hz). IR (KBr, cm^{-1}): 501(m), 693(m), 1103(m), 1434(m), 1779(vs), 1884(s), 1905(s).

($Et_2NC_2H_4PPh_2$-κ^2*N,P*)PhPt−WCp(CO)$_3$ (4). Pale yellow powder. Yield: 90%. Anal. Calcd for $C_{32}H_{34}NO_3PPtW$: C, 43.16; H, 3.85; N, 1.57. Found: C, 43.19; H, 4.18; N, 1.42. ^{1}H NMR (CD_3COCD_3): δ 1.21 (6H, t, $^3J_{H-H}$ = 7.2 Hz, Me (N-Et)), 2.6−2.9 (4H, m, C*H*$_2$-C*H*$_2$), 3.29 (4H, q, $^3J_{H-H}$ = 7.2 Hz C*H*$_2$ (N-Et)), 5.05 (5H, s, Cp), 6.4−6.6 (6H, m, *m*- and *p*-Ph (Pt-Ph)), 6.94 (4H, m, $^3J_{H-H}$ = 8.1 Hz, $^4J_{H-H}$ = 1.2 Hz, $^3J_{Pt-H}$ = 56 Hz, *o*-Ph (Pt-Ph)), 7.37−7.63 (10H, m, Ph). ^{31}P{^{1}H} NMR (CD_3COCD_3): δ 37.5 (s, $^1J_{Pt-P}$ = 4058 Hz). IR (KBr, cm^{-1}): 1104(m), 1436(m), 1780(vs), 1887(s), 1906(s).

($Et_2NC_2H_4PPh_2$-κ^2*N,P*)MePt−Co(CO)$_4$ (5). Na[Co(CO)$_4$] was used instead of Na[MoCp(CO)$_3$]. Pale yellow powder. Yield: 88%. Anal. Calcd for $C_{23}H_{27}CoNO_4PPt$: C, 41.45; H, 4.08; N, 2.10. Found: C, 41.85; H, 4.21; N, 2.08. ^{1}H NMR (C_6D_6): δ 0.79 (6H, t, $^3J_{H-H}$ = 7.2 Hz, Me (N-Et)), 0.91 (3H, d, $^3J_{P-H}$ = 4.1 Hz, $^2J_{Pt-H}$ = 73 Hz, Pt-Me), 1.79−1.93 (4H, m,

(19) Clark, H. C.; Manzer, L. E. *J. Organomet. Chem.* **1973**, *59*, 411.
(20) Ruff, J. K.; Schlientz, W. J. *Inorg. Synth.* **1957**, *15*, 192.
(21) Bianco, V. D.; Doronzo, S. *Inorg. Synth.* **1976**, *16*, 155.

CH_2-CH_2), 2.90 (2H, dq, $^2J_{H-H}$ = 14.1 Hz, $^3J_{H-H}$ = 7.2 Hz, CH_2 (N-Et)), 3.23 (2H, dq, $^2J_{H-H}$ = 14.1 Hz, $^3J_{H-H}$ = 7.2 Hz, CH_2 (N-Et)), 7.0−7.2 (6H, m, *m*- and *p*-Ph), 7.55−7.63 (4H, m, *o*-Ph). $^{31}P\{^1H\}$ NMR (C_6D_6): δ 30.7 (s, $^1J_{Pt-P}$ = 4565 Hz). IR (KBr, cm^{-1}): 1106(m), 1436(m), 1867(s), 1897(s), 1936(vs), 2017(vs).

($Et_2NC_2H_4PPh_2$-κ^2N,P)PhPt−$Co(CO)_4$ (6). Orange plates from benzene/hexane. Yield: 35%. Anal. Calcd for $C_{28}H_{29}CoNO_4PPt$: C, 46.16; H, 4.01; N, 1.92. Found: C, 46.19; H, 3.89; N, 1.96. ^1H NMR (CD_3COCD_3): δ 1.32 (6H, t, $^3J_{H-H}$ = 7.5 Hz, Me (N-Et)), 2.7−2.9 (4H, m, CH_2-CH_2), 3.33 (2H, dq $^2J_{H-H}$ = 14.4 Hz, $^3J_{H-H}$ = 7.5 Hz, CH_2 (N-Et)), 3.49 (2H, dq, $^2J_{H-H}$ = 14.4 Hz, $^3J_{H-H}$ = 7.5 Hz, CH_2 (N-Et)), 6.4−6.5 (6H, m, *m*- and *p*-Ph (Pt-Ph)), 6.91 (4H, m, $^3J_{H-H}$ = 7.8 Hz, $^4J_{H-H}$ = 1.5 Hz, $^3J_{Pt-H}$ = 49 Hz, *o*-Ph (Pt-Ph)), 7.4−7.6 (10H, m, Ph). $^{31}P\{^1H\}$ NMR (CD_3COCD_3): δ 27.3 (s, $^1J_{Pt-P}$ = 4476 Hz). IR (KBr, cm^{-1}): 1022(m), 1436(m), 1570(m), 1877(vs), 1952(vs), 2026(vs).

(tmeda-κ^2N,N')MePt−$MoCp(CO)_3$ (7). (cod)MePt−$MoCp(CO)_3$ (121.5 mg, 0.216 mmol) was placed in a Schlenk tube under nitrogen, and toluene was added. Then TMEDA (100 μL, 0.663 mmol) was added and stirred at room temperature for 5 h. After removal of all volatile matters in a vacuum, the resulting black solid was washed with hexane and recrystallized from benzene/hexane to give brown crystals of **7** in 64% yield (78.4 mg, 0.137 mmol). Anal. Calcd for $C_{15}H_{24}MoN_2O_3Pt$: C, 31.53; H, 4.23; N, 4.90. Found: C, 31.72; H, 4.12; N, 4.74. ^1H NMR (CD_3COCD_3): δ 0.07 (3H, s, $^2J_{Pt-H}$ = 74.8 Hz, Pt-Me), 2.45 (6H, s, $^3J_{Pt-H}$ = 15.6 Hz, N-Me), 2.8 (2H, m, CH_2-CH_2), 2.82 (6H, s, $^3J_{Pt-H}$ = 37.6 Hz, N-Me), 3.14 (2H, m, CH_2-CH_2), 5.17 (5H, s, Cp). IR (KBr, cm^{-1}): 594(m), 802(m), 1462(m), 1742(vs), 1781(vs), 1866(vs).

(tmeda-κ^2N,N')PhPt−$MoCp(CO)_4$ (8). The same procedure was used as described for **7**. (cod)PhPt−$MoCp(CO)_3$ was used instead of (cod)MePt−$MoCp(CO)_3$. Orange powder. Yield: 74%. ^1H NMR (CD_2Cl_2): δ 2.50 (6H, s, $^3J_{Pt-H}$ = 44.2 Hz, N-Me), 2.56 (6H, s, $^3J_{Pt-H}$ = 14.7 Hz, N-Me), 2.74 (2H, m, CH_2-CH_2), 2.98 (2H, m, CH_2-CH_2), 4.69 (5H, s, Cp), 6.72 (1H, t, $^3J_{H-H}$ = 7.2 Hz, *p*-Ph (Pt-Ph)), 6.91 (2H, t, $^3J_{H-H}$ = 7.2 Hz, *m*-Ph (Pt-Ph)), 7.23 (2H, d, $^3J_{H-H}$ = 7.2 Hz, $^3J_{Pt-H}$ = 42.1 Hz, *o*-Ph (Pt-Ph)). IR (KBr, cm^{-1}): 585(m), 799(m), 1460(m), 1775(vs), 1875(s).

($Et_2NC_2H_4PPh_2$-κ^1P)(CO)MePt−$MoCp(CO)_3$ (9). **1** (86.9 mg, 0.117 mmol) was dissolved in acetone, and the solution was degassed. Carbon monoxide (1 atm) was then introduced. After stirring for 3 h, the color of the solution was changed from orange to pale yellow. All the volatile matters were removed by evaporation, and the resulting brown-yellow solid was extracted with hexane. After the solution was concentrated under reduced pressure, the yellow solution was filtered and cooled to −30 °C to give pale yellow crystals of **9**. Yield: 58% (52.7 mg, 0.0687 mmol). Anal. Calcd for $C_{28}H_{32}MoNO_4PPt$: C, 43.76; H, 4.26; N, 1.82. Found: C, 43.94; H, 4.55; N, 1.79. Molar electrical conductivity Λ (THF, 24.5 °C): 0.24 S cm^2 mol^{-1}. ^1H NMR (C_6D_6): δ 0.95 (6H, t, $^3J_{H-H}$ = 7.2 Hz, Me (N-Et)), 1.33 (3H, d, $^3J_{P-H}$ = 8.7 Hz, $^2J_{Pt-H}$ = 61 Hz, Pt-Me), 2.39 (4H, q, $^3J_{H-H}$ = 7.2 Hz, CH_2 (N-Et)), 2.55−3.05 (4H, m, CH_2-CH_2), 4.94 (5H, s, Cp), 6.9−7.1 (6H, m, *m*- and *p*-Ph), 7.5−7.6 (4H, m, *o*-Ph). $^{31}P\{^1H\}$ NMR (C_6D_6): δ 27.4 (s, $^1J_{Pt-P}$ = 2906 Hz). $^{13}C\{^1H\}$ NMR (C_6D_6): δ 189.2 (s, $^1J_{Pt-C}$ = 1031 Hz). IR (KBr, cm^{-1}): 1841(s), 1934(s), 2039(s).

($Et_2NC_2H_4PPh_2$-κ^1P)(CO)PhPt−$MoCp(CO)_3$ (10). Complex **2** (5.8 mg, 0.072 mmol) was placed in a NMR tube, and CD_3COCD_3 (0.6 mL) was added by bulb-to-bulb distillation. Then CO (1 atm) was introduced into the NMR tube. Complex **10** was characterized spectroscopically. The compound was obtained in quantitative spectroscopic yield. ^1H NMR (C_6D_6): δ 0.80 (6H, t, $^3J_{H-H}$ = 6.9 Hz, Me (N-Et)), 2.1 (2H, m, CH_2-CH_2), 2.22 (4H, q, $^3J_{H-H}$ = 6.9 Hz, CH_2 (N-Et)), 2.6 (2H, m, CH_2-CH_2), 4.67 (5H, s, Cp), 6.68 (1H, t, $^3J_{H-H}$ = 7.5 Hz, *p*-Ph (Pt-Ph)), 6.9 (8H, m, *m*-Ph (Pt−Ph), *m*- and *p*-Ph), 7.27 (2H, d, $^3J_{H-H}$ = 7.5 Hz, *o*-Ph (Pt−Ph)), 7.4 (4H, m, *o*-Ph). $^{31}P\{^1H\}$ NMR (C_6D_6): δ 18.9 (s, $^1J_{Pt-P}$ = 2762 Hz).

($Et_2NC_2H_4PPh_2$-κ^1P)(CO)MePt−$WCp(CO)_3$ (11). The same procedure was used as described for **9**. **3** was used instead of **1**. Yellow powder. Yield: 13%. Anal. Calcd for $C_{28}H_{32}NO_4PPtW$: C, 39.27; H, 3.77; N, 1.64. Found: C, 38.94; H, 4.25; N, 1.63. ^1H NMR (C_6D_6): δ 0.94 (6H, t, $^3J_{H-H}$ = 7.2 Hz, Me (N-Et)), 1.58 (3H, d, $^3J_{P-H}$ = 8.7 Hz, $^2J_{Pt-H}$ = 61 Hz, Pt-Me), 2.40 (4H, q, $^3J_{H-H}$ = 7.2 Hz, CH_2 (N-Et)), 2.52−3.10 (4H, m, CH_2-CH_2), 4.90 (5H, s, Cp), 6.9−7.1 (6H, m, *m*- and *p*-Ph), 7.51−7.58 (4H, m, *o*-Ph). $^{31}P\{^1H\}$ NMR (C_6D_6): δ 26.8 (s, $^1J_{Pt-P}$ = 2811 Hz). IR (KBr, cm^{-1}): 694(m), 1101(m), 1435(m), 1832(vs), 1931(vs), 2037(s).

($Et_2NCH_2CH_2PPh_2$-κ^1P)(CO)PhPt−$WCp(CO)_3$ (12). The same procedure was used as described for **10**. **4** was used instead of **2**. Complex **12** was characterized spectroscopically. Yield: 89%. ^1H NMR (C_6D_6): δ 0.80 (6H, t, $^3J_{H-H}$ = 6.9 Hz, Me (N-Et)), 2.1 (2H, m, CH_2-CH_2), 2.22 (4H, q, $^3J_{H-H}$ = 6.9 Hz, CH_2 (N-Et)), 2.6 (2H, m, CH_2-CH_2), 4.61 (5H, s, Cp), 6.65 (1H, t, $^3J_{H-H}$ = 7.5 Hz, *p*-Ph (Pt-Ph)), δ 6.9 (8H, *m*-Ph (Pt-Ph), *m*- and *p*-Ph), δ 7.22 (2H, d, $^3J_{H-H}$ = 7.5 Hz, *o*-Ph (Pt-Ph)), δ 7.4 (4H, m, *o*-Ph). $^{31}P\{^1H\}$ NMR (C_6D_6): δ 17.8 (s, $^1J_{Pt-P}$ = 2674 Hz).

[PtMe(CO)(tmeda-κ^2N,N')]$^+$[$MoCp(CO)_3$]$^-$ (13). Complex **7** (5.2 mg, 0.0091 mmol) was placed in a NMR tube into which CD_3COCD_3 (0.6 mL) was added by bulb-to-bulb distillation, and then 2 equiv of TMEDA (2.7 μL, 0.018 mmol) was added. Then CO (1 atm) was introduced into the NMR tube. Complex **13** was characterized spectroscopically. Yield: 98%. ^1H NMR (CD_3COCD_3): δ 0.90 (3H, s, $^2J_{Pt-H}$ = 69.1 Hz, Pt-Me), 2.94 (6H, s, $^3J_{Pt-H}$ = 39.4 Hz, N-Me), 3.24 (6H, s, $^3J_{Pt-H}$ = 22.8 Hz, N-Me), 3.2−3.5 (4H, m, CH_2-CH_2), 4.99 (5H, s, Cp).

($Et_2NC_2H_4PPh_2$-κ^2N,P)(MeCO)Pt−$MoCp(CO)_3$ (14). The compound was prepared by the same procedure described for **1**, but characterized spectroscopically. Pt(COMe)Cl($Et_2NC_2H_4PPh_2$-κ^2N,P) was used instead of PtMeCl($Et_2NC_2H_4PPh_2$-κ^2N,P). Orange needles. Yield: 27%. ^1H NMR (C_6D_6): δ 0.83 (6H, t, $^3J_{H-H}$ = 7.2 Hz, Me (N-Et)), 1.9−2.1 (4H, m, CH_2-CH_2), 1.92 (3H, d, $^3J_{P-H}$ = 1.2 Hz, Pt-COMe), 3.15 (4H, q, $^3J_{H-H}$ = 7.2 Hz, CH_2 (N-Et)), 5.09 (5H, s, Cp), 6.99−7.14 (6H, m, *m*- and *p*-Ph), 7.68−7.75 (4H, m, *o*-Ph). $^{31}P\{^1H\}$ NMR (C_6D_6): δ 29.8 (s, $^1J_{Pt-P}$ = 4399 Hz). IR (KBr, cm^{-1}): 1040(m), 1101(m), 1437(m), 1646(s), 1782(vs), 1798(vs), 1899(s).

Time Course of Reaction of 5 with CO. Complex **5** (7.0 mg, 0.011 mmol) and Ph_3CH (5.5 mg, 0.023 mmol) as an internal standard were placed in a NMR tube into which C_6D_6 (0.5 mL) and then CO (0.1 MPa) were introduced. The acetyl and carbonyl complexes ($Et_2NC_2H_4PPh_2$-κ^2N,P)(MeCO)Pt−$Co(CO)_4$ (**15**) and ($Et_2NC_2H_4PPh_2$-κ^1P)(CO)MePt−$Co(CO)_4$ (**16**) were characterized by ^1H NMR and $^{31}P\{^1H\}$ NMR, and their amounts were periodically monitored based on the internal standard. Initially the carbonyl complex **16** was formed in 10 min in quantitative yield, and then the acetyl complex **15** was slowly formed. After 24 h at 30 °C, complex **15** was formed in 100% yield. **15**: ^1H NMR (C_6D_6): δ 0.79 (6H, t, $^3J_{H-H}$ = 6.9 Hz, Me (N-Et)), 1.7−2.0 (4H, m, CH_2-CH_2), 1.94 (3H, s, Pt-COMe), 2.76 (2H, br, CH_2 (N-Et)), 2.99 (2H, br, CH_2 (N-Et)), 7.0 (6H, m, *m*-, *p*-Ph), 7.63 (4H, m, *o*-Ph). $^{31}P\{^1H\}$ NMR (C_6D_6): δ 21.9 (s, $^1J_{Pt-P}$ = 4797 Hz). IR (KBr, cm^{-1}): 1103(m), 1436(m), 1644(m), 1888(vs), 1948(vs), 2029(s). **16**: ^1H NMR (C_6D_6): δ 0.87 (6H, t, $^3J_{H-H}$ = 7.2 Hz, Me (N-Et)), 1.04 (3H, d, $^3J_{P-H}$ = 6.6 Hz, $^2J_{Pt-H}$ = 73 Hz, Pt-Me) 2.32 (4H, q, $^3J_{H-H}$ = 7.2 Hz, CH_2 (N-Et)), 2.5 (2H, m, CH_2-CH_2), 2.8 (2H, m, CH_2-CH_2), 7.0−7.5 (10H, m, Ph). $^{31}P\{^1H\}$ NMR (C_6D_6): δ 19.0 (s, $^1J_{Pt-P}$ = 3394 Hz).

[PtMe($Et_2NC_2H_4PPh_2$-κ^1P)($Et_2NC_2H_4PPh_2$-κ^2N,P)]$^+$[$MoCp(CO)_3$]$^-$ (17). To a solution of **1** (73.1 mg, 0.099 mmol) in a minimum quantity of toluene (ca. 1 mL) was added $Et_2NC_2H_4PPh_2$ (22 μL, 0.103 mmol) at −30 °C, and the solution was stirred for 1 day at room temperature. Then hexane (ca. 20 mL) was added to precipitate an analytically pure pale

yellow powder of **17**, which was filtered, washed with hexane, and dried under vacuum at room temperature. Yield: 75% (76.7 mg, 0.075 mmol). Anal. Calcd for $C_{45}H_{56}MoN_2O_3P_2Pt$: C, 52.68; H, 5.50; N, 2.73. Found: C, 53.04; H, 5.63; N, 2.46. Molar electrical conductivity Λ (THF, 21 °C): 12.6 S cm^2 mol^{-1}. ^{1}H NMR (CD_3COCD_3): δ 0.55 (3H, dd, $^3J_{P-H}$ = 5.1, 3.3 Hz, $^2J_{Pt-H}$ = 51 Hz, Pt-Me), 0.87 (6H, t, $^3J_{H-H}$ = 7.2 Hz, Me (N-Et)), 1.42 (6H, t, $^3J_{H-H}$ = 6.9 Hz, Me (Pt-N-Et)), 2.38 (4H, q, $^3J_{H-H}$ = 7.2 Hz, CH_2 (N-Et)), 2.4−3.1 (8H, m, CH_2-CH_2), 3.3 (2H, m, CH_2 (Pt-N-Et)), 3.5 (2H, m, CH_2 (Pt-N-Et)), 4.96 (5H, s, Cp), 7.2−7.7 (20H, m, Ph). ^{31}P{^{1}H} NMR (CD_3COCD_3): δ 5.3 (d, $^2J_{P-P}$ = 12 Hz, $^1J_{Pt-P}$ = 3741 Hz), 46.6 (d, $^2J_{P-P}$ = 12 Hz, $^1J_{Pt-P}$ = 1962 Hz). IR (KBr, cm^{-1}): 800(m), 1022(m), 1102(m), 1261(m), 1435(m), 1763(s), 1892(s).

The following complexes **18**−**21** were prepared analogously.

[PtMe(PMe$_3$)(Et$_2$NC$_2$H$_4$PPh$_2$-κ^2*N,P*)]$^+$[MoCp(CO)$_3$]$^-$ (18). Pale yellow powder. Yield: 75%. Anal. Calcd for $C_{30}H_{41}MoNO_3P_2Pt$: C, 44.12; H, 5.06; N, 1.72. Found: C, 43.82; H, 4.98; N, 1.64. ^{1}H NMR (CD_3COCD_3): δ 0.64 (3H, dd, $^3J_{P-H}$ = 6.9, 3.0 Hz, $^2J_{Pt-H}$ = 52 Hz, Pt-Me), 1.29 (6H, t, $^3J_{H-H}$ = 7.2 Hz, Me (N-Et)), 1.44 (9H, d, $^3J_{P-H}$ = 11.4 Hz, $^2J_{Pt-H}$ = 56 Hz, PMe$_3$), 2.7−3.05 (4H, m, CH_2-CH_2), 3.1−3.5 (4H, m, CH_2 (N-Et)), 4.96 (5H, s, Cp), 7.65−7.71 (6H, m, *m*- and *p*-Ph), 7.89−7.96 (4H, m, *o*-Ph). ^{31}P{^{1}H} NMR (CD_3COCD_3): δ −27.1 (d, $^2J_{P-P}$ = 13 Hz, $^1J_{Pt-P}$ = 3531 Hz), 46.0 (d, $^2J_{P-P}$ = 14 Hz, $^1J_{Pt-P}$ = 1935 Hz).

[PtMe(PEt$_3$)(Et$_2$NC$_2$H$_4$PPh$_2$-κ^2*N,P*)]$^+$[MoCp(CO)$_3$]$^-$ (19). White yellow powder. Yield: 93%. Anal. Calcd for $C_{33}H_{47}MoNO_3P_2Pt$: C, 46.16; H, 5.52; N, 1.63. Found: C, 45.72; H, 5.32; N, 1.59. ^{1}H NMR (CD_3COCD_3): δ 0.11 (3H, dd, $^3J_{P-H}$ = 6.9, 3.0 Hz, $^2J_{Pt-H}$ = 51 Hz, Pt-Me), 1.44 (9H, dt, $^3J_{H-H}$ = 7.5 Hz, $^3J_{P-H}$ = 17.4 Hz, Me (PEt$_3$)), 1.30 (6H, t, $^3J_{H-H}$ = 7.2 Hz, Me (N-Et)), 1.70 (6H, dq, $^3J_{H-H}$ = 7.5 Hz, $^3J_{P-H}$ = 9.6 Hz, CH_2 (PEt$_3$)), 3.2 (2H, m, CH_2 (N-Et)), 3.5 (2H, m, CH_2 (N-Et)), 2.7−3.0 (4H, m, CH_2-CH_2), 4.97 (5H, s, Cp), 7.6−7.7 (6H, m, *m*- and *p*-Ph), 7.85−7.9 (4H, m, *o*-Ph). ^{31}P{^{1}H} NMR (CD_3COCD_3): δ 8.1 (d, $^2J_{P-P}$ = 14 Hz, $^1J_{Pt-P}$ = 3576 Hz), 45.4 (d, $^2J_{P-P}$ = 14 Hz, $^1J_{Pt-P}$ = 1819 Hz). IR (KBr, cm^{-1}): 774(m), 1103(m), 1436(m), 1763(vs), 1887(vs).

[PtMe(PPh$_3$)(Et$_2$NC$_2$H$_4$PPh$_2$-κ^2*N,P*)]$^+$[MoCp(CO)$_3$]$^-$ (20). Pale yellow powder. Yield: 77%. Anal. Calcd for $C_{46}H_{48}MoNO_3P_2Pt$: C, 54.39; H, 4.76; N, 1.38. Found: C, 54.10; H, 4.65; N, 1.38. ^{1}H NMR (CD_3COCD_3): δ 0.11 (3H, dd, $^3J_{P-H}$ = 6.3, 3.3 Hz, Pt-Me), 1.45 (6H, t, $^3J_{H-H}$ = 6.9 Hz, Me (N-Et)), 2.9−3.1 (4H, m, CH_2-CH_2), 3.35 (2H, m, CH_2 (N-Et)), 3.62 (2H, m, CH_2 (N-Et)), 4.97 (5H, s, Cp), 7.28−7.62 (25H, m, Ph). ^{31}P-{^{1}H} NMR (CD_3COCD_3): δ 16.3 (d, $^2J_{P-P}$ = 12 Hz, $^1J_{Pt-P}$ = 3876 Hz), 48.1 (d, $^2J_{P-P}$ = 12 Hz, $^1J_{Pt-P}$ = 2004 Hz).

[PtMe{P(OMe)$_3$}(Et$_2$NC$_2$H$_4$PPh$_2$-κ^2*N,P*)]$^+$[MoCp(CO)$_3$]$^-$ (21). White yellow plate. Yield: 32% after recrystallization from THF/ether. Anal. Calcd for $C_{30}H_{41}MoNO_6P_2Pt$: C, 41.67; H, 4.78; N, 1.62. Found: C, 41.47; H, 4.65; N, 1.58. ^{1}H NMR (CD_3COCD_3): δ 0.67 (3H, dd, $^3J_{P-H}$ = 6.6, 1.2 Hz, $^2J_{Pt-H}$ = 51 Hz, Pt-Me), 1.34 (6H, t, $^3J_{H-H}$ = 6.9 Hz, Me (N-Et)), 2.8−3.3 (4H, m, CH_2-CH_2), 3.3 (2H, m, CH_2 (N-Et)), 3.4 (2H, m, CH_2 (N-Et)), 3.54 (9H, d, $^3J_{P-H}$ = 12.9 Hz, P(OMe)$_3$), 4.96 (5H, s, Cp), 7.60−7.64 (6H, m, *m*- and *p*-Ph), 7.76−7.83 (4H, m, *o*-Ph). ^{31}P{^{1}H} NMR (CD_3COCD_3): δ 50.6 (d, $^2J_{P-P}$ = 21 Hz, $^1J_{Pt-P}$ = 1836 Hz), 87.6 (d, $^2J_{P-P}$ = 21 Hz, $^1J_{Pt-P}$ = 6186 Hz).

[*trans*-PtMe(PPh$_3$)(Et$_2$NC$_2$H$_4$PPh$_2$-κ^2*N,P*)]$^+$[MoCp(CO)$_3$]$^-$ (22). Complex **22** was characterized spectroscopically. Yield: 97%. ^{1}H NMR (CD_3COCD_3): δ 0.17 (3H, dd, $^3J_{P-H}$ = 8.1, 6.6 Hz, Pt-Me), 1.02 (6H, t, $^3J_{H-H}$ = 6.9 Hz, Me (N-Et)), 2.6−3.0 (8H, m, CH_2-CH_2 and CH_2 (N-Et)), 4.97 (5H, s, Cp), 7.2−8.0 (25H, m, Ph). ^{31}P{^{1}H} NMR (CD_3COCD_3): δ 31.9 (d, $^2J_{P-P}$ = 405 Hz, $^1J_{Pt-P}$ = 2975 Hz), 43.0 (d, $^2J_{P-P}$ = 405 Hz, $^1J_{Pt-P}$ = 3239 Hz).

[PtMe(PPh$_3$)(dppe-κ^2*P,P′*)]$^+$[MoCp(CO)$_3$]$^-$ (23). To a solution of (dppe-κ^2*P,P′*)MePt−MoCp(CO)$_3$ (87.5 mg, 0.103 mmol) in a minimum quantity of toluene (ca. 1 mL) was added PPh$_3$ (39.4 mg, 0.150 mmol), and the solution was stirred for 3 day at room temperature. Then hexane (ca. 20 mL) was added to precipitate a pale yellow powder of **23**, which was filtered, washed with hexane, and recrystallized from CH_2Cl_2/hexane to give pale yellow crystals in 86% yield (98.7 mg, 0.0885 mmol). ^{1}H NMR (CD_3COCD_3): δ 0.55 (3H, q, $^3J_{P-H}$ = 6.3 Hz, $^2J_{Pt-H}$ = 58.8 Hz, Pt-Me), 2.4−2.8 (4H, m, CH_2-CH_2), 4.98 (5H, s, Cp), 7.2−7.8 (35H, m, Ph). ^{31}P{^{1}H} NMR (CD_3COCD_3): δ 26.7 (dd, $^2J_{P-P}$ = 380, 17 Hz, $^1J_{Pt-P}$ = 2769 Hz), 50.6 (dd, $^2J_{P-P}$ = 17, 5 Hz, $^1J_{Pt-P}$ = 1824 Hz), 54.5 (dd, $^2J_{P-P}$ = 380, 5 Hz, $^1J_{Pt-P}$ = 2743 Hz). IR (KBr, cm^{-1}): 690(m), 110-(m), 1436(m), 1767(vs), 1897(vs).

Reaction of 7 with PPh$_3$. Complex **7** (6.3 mg, 0.011 mmol) was placed in a NMR tube, and CD_3COCD_3 (0.6 mL) was added by bulb-to-bulb distillation. Then PPh$_3$ (9.4 mg, 0.035 mmol) was introduced into the NMR tube. Two ionic complexes, [PtMe(PPh$_3$)(tmeda-κ^2*N,N′*)]$^+$[MoCp(CO)$_3$]$^-$ (**24**) and [PtMe-(PPh$_3$)$_3$]$^+$[MoCp(CO)$_3$]$^-$ (**25**), were characterized by ^{1}H and ^{31}P-{^{1}H} NMR. Yield: 12% (**24**) and 88% (**25**). **24**: ^{1}H NMR (CD_3COCD_3): δ 0.27 (3H, d, $^3J_{P-H}$ = 3.3 Hz, $^2J_{Pt-H}$ = 68.5 Hz, Pt-Me), 2.35 (6H, s, N-Me), 2.94 (6H, d, $^4J_{P-H}$ = 3.0 Hz, $^3J_{Pt-H}$ = 33.6 Hz, N-Me), 2.9−3.2 (4H, m, CH_2-CH_2), 4.98 (s, Cp), Ph resonances of PPh$_3$ ligand obscured by signals due to **25** and free PPh$_3$. ^{31}P{^{1}H} NMR (CD_3COCD_3): δ 18.5 (s). **25**: ^{1}H NMR (CD_3COCD_3): δ 0.34 (3H, dt, $^3J_{P-H}$ = 8.1, 5.7 Hz, $^2J_{Pt-H}$ = 56.5 Hz, Pt-Me), 4.98 (s, Cp), Ph resonances of PPh$_3$ ligand obscured by signals due to **24** and free PPh$_3$. ^{31}P{^{1}H} NMR (CD_3COCD_3): δ 20.8 (t, $^2J_{P-P}$ = 20 Hz, $^1J_{Pt-P}$ = 1937 Hz), 28.7 (d, $^2J_{P-P}$ = 20 Hz, $^1J_{Pt-P}$ = 2937 Hz).

X-ray Structure Determinations. A single crystal was selected by using a monochromated microscope and sealed in a thin-glass capillary (GLAS, 0.7 mm ϕ) under N_2. Diffraction experiments were performed on a Rigaku RASA-7R diffractometer with graphite-monochromated Mo Kα radiation (λ = 0.71069 Å) and a rotating anode generator. The intensities of three representative reflections were measured after every 150 reflections. No decay correction was applied for **21**. These structures were solved by direct methods, expanded using Fourier techniques,[22] and refined by full-matrix least squares. For complex **2**, all non-hydrogen atoms were refined with anisotropic displacement parameters except for the Cp ring, and the incorporated solvent molecule was treated as rigid groups. All hydrogen atoms were included in theoretical positions. All non-hydrogen atoms for **21** were anisotropic, and the hydrogen atoms were included in theoretical positions. These data were processed using the teXsan crystal solution package[23] operating on a SGI O_2 workstation. The crystallographic data and details associated with data collection for **2** and **21** are given in Table 1. Crystallographic thermal parameters and bond distances and angles have been deposited as Supporting Information.

Acknowledgment. This work was financially supported by a Grant-in-Aid for Scientific Research from the Ministry of Education, Sports, Culture, Science and Technology, Japan, and the 21st Century COE (Center of Excellence) program of "Future Nano-materials" at Tokyo University of Agriculture and Technology.

Supporting Information Available: Tables of atomic coordinates, anisotropic displacement parameters, and bond distances and angles for **2** and **21**. This material is available free of charge via the Internet at http://pubs.acs.org.

OM030477U

(22) DIRDIF94: Beurskens, P. T.; Admiraal, G.; Beurskens, G.; Bosman, W. P.; de Gelder, R.; Israel, R.; Smits, J. M. M. *The DIRDIF-94 Program System*; Technical Report of the Crystallography Laboratory; University of Nijmegen: The Netherlands, 1994.

(23) *teXsan*: Crystal Structure Analysis Package; Molecular Structure Corp.: The Woodlands, TX, 1985 and 1992.